Dyes and Pigments 95 (2012) 79–88

Contents lists available at SciVerse ScienceDirect

Dyes and Pigments

journal homepage: www.elsevier.com/locate/dyepig

A new heterogeneous catalytic system for decolorization and mineralization of Orange G acid dye based on hydrogen peroxide and a macroporous chelating polymer

Viorica Dulman [a], Simona Maria Cucu-Man [a], Romeo Iulian Olariu [a], Rodica Buhaceanu [a], Mihai Dumitraş [a], Ion Bunia [b,*]

[a] *University "Al. I. Cuza", Faculty of Chemistry, 11 Carol I Bd., 700506 Iasi, Romania*
[b] *"P. Poni" Institute of Macromolecular Chemistry, 41A Grigore Ghica Voda Alley, 700487 Iasi, Romania*

ARTICLE INFO

Article history:
Received 14 December 2011
Received in revised form
19 March 2012
Accepted 22 March 2012
Available online 29 March 2012

Keywords:
Decolorization
Orange G
Catalytic decolorization
Heterogeneous catalyst
Mineralization
Macroporous chelating polymer

ABSTRACT

The decolorization and the mineralization of the Orange G dye in aqueous solutions with hydrogen peroxide in a heterogeneous system, involving a new catalyst, obtained by the adsorption of Cu(II) ions onto a macroporous chelating polymer functionalized with diethylenetriamine, was investigated. Special attention has been paid to the effect of solution pH, H_2O_2 and dye concentration, reaction time, temperature and amount of catalyst on the decolorization efficiency of Orange G containing water. The decolorization kinetics of Orange G by this catalytic system was also elucidated, based on experimental data. The oxidation reaction was found to follow pseudo-first-order kinetics with respect to dye concentration. The rate constants for temperatures ranging from 24 to 50 °C and the activation parameters were calculated. Activation energy, as well as activation enthalpy and entropy were calculated using the Arrhenius and Eyring equations, respectively. The new tested catalyst displayed good stability and was efficient for the decolorization and mineralization of Orange G dye under mild reaction conditions. Complete color removal was achieved in 30 min at 24 °C and in 15 min at 50 °C ($pH = 7$, $[H_2O_2] = 130$ mmol L^{-1}, in the presence of 0.06 g of the catalyst) at an initial dye concentration of 50 mg L^{-1}. The tested heterogeneous catalyst is a new cost effective alternative for the treatment of wastewaters containing Orange G dye.

1. Introduction

Industrial discharge of effluents containing dyes influences the natural aspect of rivers and has a negative impact upon aquatic life because of interference with the transmission of sunlight which diminishes the action of photosynthesis. In addition, some azo dyes and their degradation products are highly toxic and even carcinogenic [1]. Azo dyes with one or more azo groups (−N=N−) constitute the largest and the most diverse group of synthetic dyes. They are widely used in various industries, such as those producing textiles, foods, cosmetics and paper printing and are generally resistant to biodegradation due to their xenobiotic nature [2–5].

Orange G (OG) is a synthetic azo dye used in different domains, such as in histology in many staining formulations, and as a dye for textiles (wool and silk), paper, leather, wood stain, coloring inks and copying pencils. Extended exposure to this dye may lead to irritation of the respiratory and gastrointestinal tract. It also affects anaerobic biomass in aqueous solutions [6]. Therefore, various physical or chemical treatment processes for dyes from wastewaters have been tested [7,8].

Among the methods applied for OG decolorization, one can first refer to biological processes [2]. The *Bacillus fusiformis* (strain KMK5) bacteria can decolorize and degrade the OG dye [9]. The strains of wood-rot fungi have a similar action upon OG azo dye [10–14]. Reductive cleavage of azo bonds, leading to the formation of aromatic amines, constitutes the initial reaction in the bacterial metabolism of azo dyes. The subsequent degradation of aromatic amines depends on their chemical structure and experimental conditions [3].

The photodegradation of the OG azo dye has also been investigated under various conditions, such as: UV-irradiated titania [15], modified titania [16], solar photocatalytic cells with nano-TiO_2 [17], nano-sized Sn(IV)/TiO_2/AC photocatalyst [18], fluidizing carrier with immobilized TiO_2 [19], Pd substituted nano-TiO_2 [20], and by nitrogen-doped TiO_2 nanocatalysts [21]. For example, the commercial TiO_2 known as P25, showed a high photocatalytic activity under

---

* Corresponding author. Tel.: +40 2322217454; fax: +40 232211299.
E-mail address: ibunia@icmpp.ro (I. Bunia).

0143-7208/$ – see front matter © 2012 Elsevier Ltd. All rights reserved.
doi:10.1016/j.dyepig.2012.03.024

sunlight. The photosensitive oxidation mechanism of OG was also thought to be contributing to the higher visible-light-induced decolorization efficiency.

The interactive oxidation by photoelectrocatalysis and electro–Fenton catalysis for azo dye decolorization (including OG), using TiO_2–Ti mesh and reticulated vitreous carbon electrodes, was also studied [22]. OG was completely oxidized and removed electrochemically using graphite electrodes under certain conditions of initial pH and current density [6].

The decolorization of resistant dyes with hydrogen peroxide by a heterogeneous catalytic reaction is one of the most effective methods for the wastewater treatment. This method consists of using catalysts, such as: silica, alumina and cation exchange resins in the form of transition metal complexes. The reactivity of the catalysts is correlated with the redox potential of metal ions, the amount of the complex on catalytic support, the type of the support and the structure of the dye.

The most common homogeneous catalytic methods for pollutant degradation use Fe^{2+}, which is referred to as Fenton's reagent when used in combination with H_2O_2. Notable examples and discussions of the heterogeneous catalytic Fenton system for synthetic dye removal are in an excellent comprehensive review [4]. Decolorization of OG in aqueous solution by Fenton and Fenton-like systems was discussed in detail by other authors [23,24].

Copper can also be used as a catalyst, preferably in a heterogeneous system. Copper is known to undergo Fenton-type reaction and has been used as an activator in the decomposition of H_2O_2 and in the degradation of various dyes [25,26]. The suggested mechanism claims that the catalyst activates the H_2O_2 molecules, leading to the formation of hydroxyl radicals, $\cdot OH$ [27–29]. The latter attacks the dyes forming an active intermediate, which decomposed itself in the rate determining step giving the final oxidation products, as shown in the following equations scheme:

$$S-\left[M^{II}L_n\right]^{2+}+H_2O_2 \underset{k_{-1}}{\overset{k_1}{\rightleftarrows}} S-\left[M^{II}L_n\left(HO_2^-\right)\right]^{+}+H^{+} \tag{1}$$

peroxo complex

$$S-\left[M^{II}L_n\left(HO_2^-\right)\right]^{+} \xrightarrow{k_2} S-\left[M^{I}L_n\right]^{+}+\cdot OH+1/2O_2 \tag{2}$$

$$\text{Dye}+\cdot OH \xrightarrow{k_3} \text{Intermediate} \tag{3}$$

$$\text{Intermediate} \xrightarrow{k_4} \text{oxidation products}+CO_2 \tag{4}$$

$$S-\left[M^{I}L_n\right]^{+}+\cdot OH \xrightarrow{k_5} S-\left[M^{II}L_n\right]^{2+}+OH^{-} \tag{5}$$

$$OH^{-}+H^{+}\rightarrow H_2O$$

where S is the polymeric support, L the ligand and M the metal ions.

The aim of this paper is the investigation of the degradation process of the OG dye using H_2O_2 in a heterogeneous system, involving a new catalyst obtained by the adsorption of Cu(II) ions onto a macroporous chelating polymer functionalized with diethylenetriamine (DETA), catalyst denoted Cu(II)-A. The effect of pH, H_2O_2 and dye concentration, temperature, amount of catalyst, and the stability of the catalyst on the decolorization of the OG were evaluated in detail. Furthermore, the decolorization kinetics of OG by the proposed catalytic system was elucidated based on experimental data. The rate constants for temperatures ranging from 24 to 50 °C and the activation parameters were calculated. To the best of our knowledge, this is the first time when this catalytic system was tested on the decolorization of the OG, as a new cost effective alternative for the treatment of wastewaters containing OG dye.

2. Materials and methods

2.1. Dye

The monoazo dye OG, as sulfonic acid sodium salt (Scheme 1), purchased from Aldrich, dye content 95%, was used without any prior purification.

Aqueous dye solutions of 1 g L^{-1} were prepared using double distilled water, subsequently diluted when necessary. The concentration of this solution corresponds to 2.1 10^{-3} mol L^{-1}, related to pure dye content.

2.2. Hydrogen peroxide

Hydrogen peroxide ~30% H_2O_2 (Merck) was used. Prior to each use, the concentration of H_2O_2 was determined iodometrically using a standardized solution of sodium thiosulphate.

2.3. Catalyst

The catalyst was obtained by the adsorption of Cu(II) onto a weak basic exchanger in four steps, as following:

1. Firstly, a crosslinked acrylic copolymer containing 10% divinylbenzene (DVB), 10% vinyl acetate (VAc), and 80% acrylonitrile (AN) was synthesized by radical copolymerization. The reaction has been conducted in aqueous suspension, in an inert medium (toluene), using benzoyl peroxide as initiator (1 wt%) and ammonium salt of poly(styrene-co-maleic anhydride) as polymeric stabilizer in the aqueous phase (0.5 wt%). The aqueous/organic phase ratio was 3:1 (v/v). The reaction was allowed to proceed for 4 h at 65 °C, 6 h at 75 °C, and 8 h at 85 °C. After polymerization, the copolymer beads were washed with warm water and then extracted with dichlorethane in a Soxhlet apparatus to remove traces of residual monomers, linear oligomers and toluen. Finally the copolymer beads were vacuum dried at 50 °C for 48 h.
2. The functionalization of this polymer was performed with DETA, following a polymer–analog reaction, at 110 °C, during 8 h [30]. Fig. 1 shows the chemical structure of the functionalized polymer (A) and Table 1 summarized some of its characteristics.
3. The functionalized weak basic resin (in the shape of spherical beads) was further treated with NaOH (1 mol L^{-1}) and then thoroughly washed with double distilled water and air dried. Thus, the primary amino groups $-NH_2$ were transformed into free basic form, $-NH_3^+-OH^-$.
4. The polymer was swelled with double distilled water, at room temperature, for 24 h. The saturation of chelating resins with Cu(II) ions was obtained at pH = 5.2 by adding an excess of

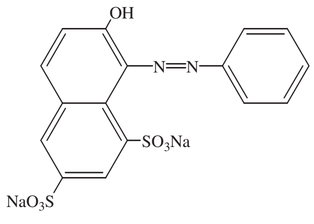

Scheme 1. The chemical structure of Orange G.

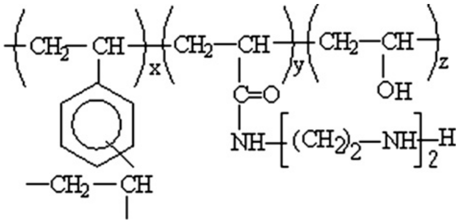

Fig. 1. The chemical structure of the functionalized polymer A: $x = 10\%$; $y = 80\%$, $z = 10\%$.

0.1 mol L^{-1} $CuSO_4 \cdot 5H_2O$ solution to the functionalized polymer and leaving it for reaction for 24 h to reach the equilibrium. The resulting product (Cu(II)-A) was thoroughly washed with double distilled water, until the solution was free of any excess of metal ions. The amount of Cu(II) retained by the functionalized polymer was calculated taking into account the concentration of the ions left in the solution, determined by flame atomic absorption spectrometry (FAAS, Perkin Elmer 3300). The amount of Cu (II) released into the solution from the catalyst in certain conditions was determined by the same method.

The surface and internal texture of the functionalized polymer, before and after Cu(II) ion adsorption, was studied with a LEITZ scanning electron microscope (SEM), using an acceleration voltage of 10 kV. The samples were fixed with colloidal silver on aluminum support and then covered with a thin gold layer. The chemical composition of the polymer A and Cu(II)-A catalyst was evaluated by infrared spectroscopy by using a Vertex 70 Bruker FTIR spectrometer. Transmission spectra were recorded in KBr pellets using a standard sample holder.

Other chelating acrylic resins, containing 3% divinylbenzene (DVB), 20% acrylonitrile (AN) and 77% ethylacrylate (EA) were prepared as described in ref [30]. The functionalization of this polymer was performed with two amines, namely with ethylenediamine (EDA), resulting the functionalized polymer denoted A1, or with triethylenetetramine (TETA), polymer denoted A2 [31]. The saturation of the chelating resins A1 and A2 was performed with 0.1 mol L^{-1} $CuSO_4 \cdot 5H_2O$ aqueous solutions, and then were tested for the decolorization of OG dye. Table 2 lists the pH conditions in which their saturation with Cu(II) ions took place.

2.4. Decolorization procedure

Different amounts of catalyst were added to a known volume of dye (20 mL for the pH effect study and 50 mL for the other experiments) with a given pH and H_2O_2 solution, specified later for each experiment. Samples of 1–2 mL (depending on the initial concentration of dye) were withdrawn at given time and after appropriate dilution the solution absorbance was determined at maximum wavelength $\lambda_{max} = 485$ nm, characteristic for OG dye. In parallel, the effects of pH and H_2O_2 concentration on the dye solution absorbance, in the absence of catalysts, were investigated. The kinetic study of the decolorization procedure was performed at constant temperature. The UV–vis spectra of OG solutions before and after decolorization and their change during catalytic decolorization were recorded using a PharmaSpec UV-1700 Shimadzu UV–vis spectrophotometer.

Table 1
Some characteristics of the functionalized polymer A.

Parameters	Values
Beads size:	0.3 – 0.8 mm
Porosity area:	$S = 55\ m^2\ g^{-1}$
Apparent density:	$\rho_{ap} = 0.719$ g/ml
Porosity:	P = 37%
Exchange capacity:	$Cs = 1.848\ meq\ mL^{-1} = 10.467\ meq\ g^{-1}$

Table 2
The saturation of ion exchangers with metal ions, at 25 °C.

Polymer	M(II)-polymer	pH	M(II)/dry polymer mmol g^{-1}
AS-55	Cu(II)-A	5.22	6.95
A1	Cu(II)-A1	3.03	2.43

2.5. CO_2 determination

CO_2 resulted during the decolorization of the dye was captured in $Ba(OH)_2$ solution and further determined gravimetrically as precipitated $BaCO_3$ [32].

2.6. Total organic carbon

Total organic carbon (TOC) was measured in the aqueous solutions resulting from the oxidative treatment using an Analytik Jena 3100 TOC/TN analyzer. Reported TOC values represent the average of at least two measurements. Before TOC measurements the reaction was stopped by adding an excess of Na_2SO_3 which quickly consumes the unreacted H_2O_2.

3. Results and discussion

3.1. Catalyst selection and characterization

Initially we tested the catalytic capacity of some products resulting from the saturation of some weak basic ion exchangers, described in ref [31], treated with Fe(II), Fe(III), Cu(II), Co(II), Mn(II) metallic ions, during the process of decolorization of several acid dyes with H_2O_2. The experimental tests showed that OG dye is stable to oxidative decolorization of the tested catalysts, except Cu(II)-A, Cu(II)-A1. The most effective catalyst is Cu(II)-A. Cu(II)-A1 acts very slowly; a long time is needed for a complete decolorization. Obviously, the different behavior of the Cu(II)-polymers as catalysts in dye decolorization is determined by the nature of the amine used for copolymer functionalization, the metallic ion, the structure of the polymeric support and also by the applied method.

The resin A, functionalized with DETA, is able to form stable complexes with metallic ions and a high affinity for Cu(II), comparative with A1, was observed (Table 2). The adsorption capacity of certain metallic ions is mainly due to the complexation process of the N atoms from the functional groups. This process is enhanced by the permanent porosity (Table 1) of this type of exchangers which offers a larger contact surface. This cation exchanger is also more hydrophilic than other types of exchanger due to the presence of –OH groups resulting from the hydrolysis of vinyl acetate.

Fig. 2 shows some SEM micrographs of the surface and the fracture of some of beads of DETA functionalized polymer A, before and after Cu(II) adsorption.

The SEM micrographs in Fig. 2a and c show that the functionalized polymer is characterized by a relatively uniform surface and with certain microstructures; a system of cavities that differ in aspect and distribution are evident as the internal texture. After Cu(II) adsorption (Fig. 2b and d), the morphological characteristics are modified on both the external and internal surface with a more irregular microstructure being evident.

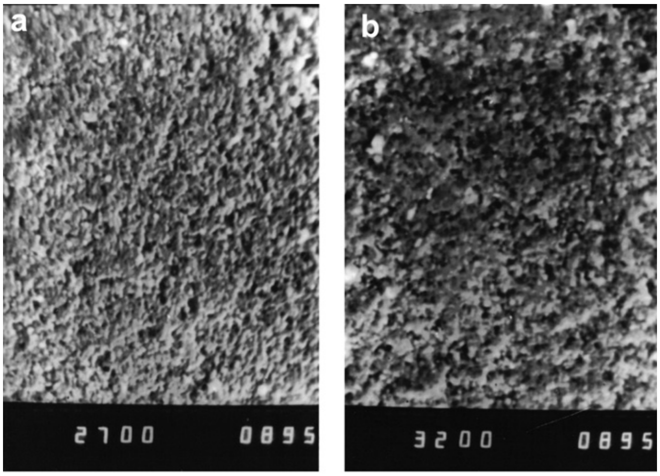

A surface Cu(II)-A surface

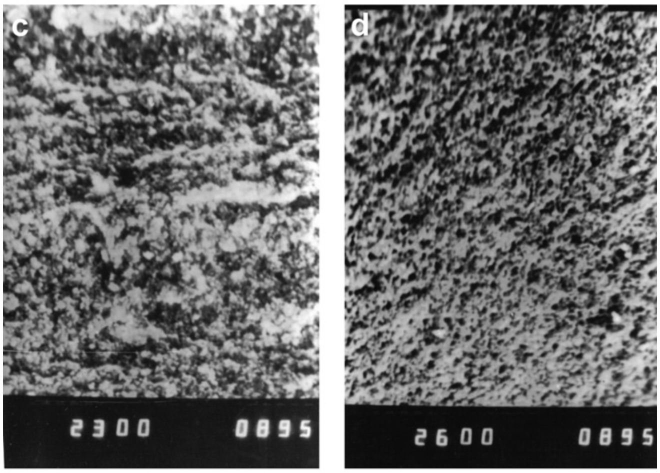

A fracture Cu(II)-A fracture

Fig. 2. SEM micrographs of functionalized polymer A: before (a,c) and after Cu(II) sorption (b,d).

The chemical composition of the polymer A and Cu(II)-A catalyst was evaluated by infrared spectroscopy (Fig. 3).

As Fig. 3 shows, the FTIR spectrum of the polymer A shows the following characteristic bands [33]: the absorption peak at 3424 cm^{-1}, characteristic of $\nu_{O-H,}$ ν_{N-H} stretching vibrations; the doublet at 3424–3297 cm^{-1} and 3426–3278 cm^{-1}, specific for the absorption peak of NH_2 group; the characteristic peaks for the amide I and II groups at 1651 and 1551 cm^{-1}. After Cu(II) adsorption, the FTIR spectrum of the Cu(II)-A shows some important changes at 610 cm^{-1} ($\nu_{Cu(II)-N}$ stretch) and at 1114 cm^{-1} $\sigma_{N-Cu(II)}$ corresponding to the formation of Cu(II)–N bonds [34].

3.2. Effect of pH

In the decolorization and mineralization experiments, the pH value of the dye solution has significant influence on the catalytic system efficiency because: (i) it can affect the catalyst stability and (ii) it influences the catalytic reaction which controls the production rate of hydroxyl radicals [35].

In order to find the optimum pH for the decolorization of OG, a series of experiments at initial pH values in the range 3–10 was conducted. At a pH between 1 and 2 a release of Cu(II) in the solution was noticed, thus no decolorization determination were performed in that pH range. Fig. 4 shows the variation of final pH and decolorization degree as a function of initial pH, under the following experimental conditions: $[OG]_0 = 50$ mg L^{-1}; $[H_2O_2]_0 = 130$ mmol L^{-1}, 0.04 g catalyst, total volume 20 mL, after 30 min reaction time.

As Fig. 4 shows, the increase in initial pH of OG solution from 3 to 4 sharply enhances the efficiency of decolorization of OG from 3% up to 97.7%; after that a very slow increase of the decolorization degree can be notice, reaching the 100% value at pH greater than 7. For the next experiments pH 7 was used, to ensure mild conditions of reaction. Fig. 4 shows that after the decolorization process the final pH values are almost constant (5.3–5.8), irrespective of the initial pH values. Moreover, when the initial pH was greater than 6, the decrease of the pH at the final time of decolorization process suggests that the decolorization of the OG dye by partial decolorization into acidic lower molecular weight species occurred.

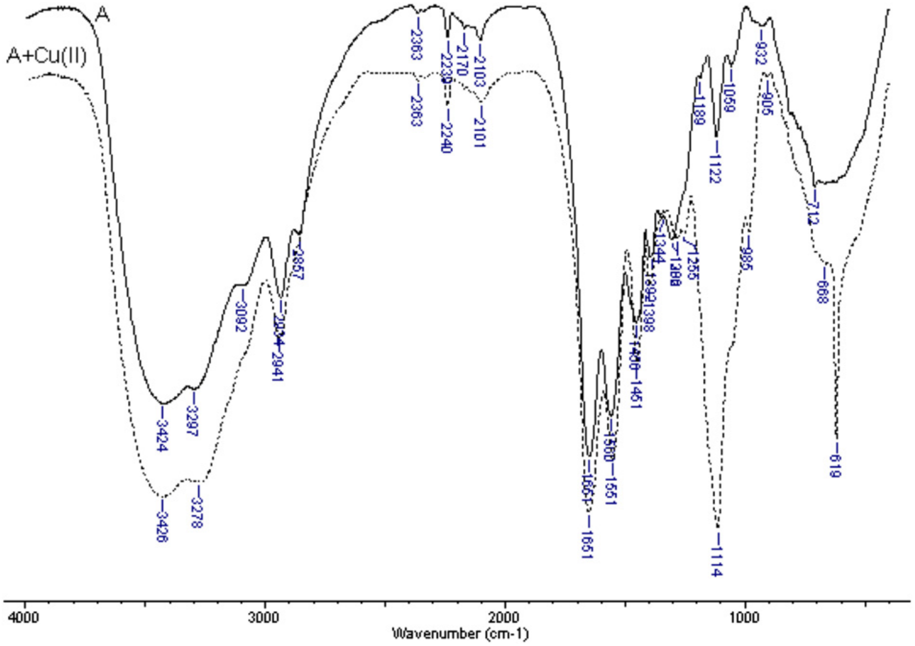

Fig. 3. FTIR spectra of functionalized polymer A, before and after Cu(II) ions adsorption.

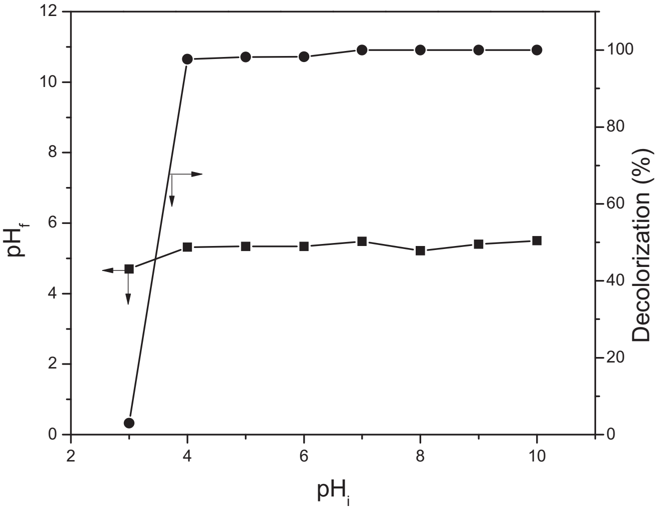

Fig. 4. The effect of the initial pH on the final pH (■) and on the decoloration degree (●) of OG solutions. Experimental conditions: $[OG]_0 = 50$ mg L^{-1}; $[H_2O_2]_0 = 130$ mmol L^{-1}; 0.04 g catalyst; 30 min reaction time.

3.3. *Effect of initial concentration of H_2O_2*

The effect of H_2O_2 concentration at the previously established optimum pH = 7 was studied in the range 10–200 mmol L^{-1} (Fig. 5).

As can be seen in Fig. 5, significant decolorization occurs even for low H_2O_2 concentrations (10 mmol L^{-1}), in 15 min. Increasing the concentration of H_2O_2 from 10 to 130 mmol L^{-1}, leads to a significant increase in the decolorization efficiency up to 94–100% and a constant level is reached after that. Also, for the same H_2O_2 concentration, the decolorization efficiency increased with the reaction time.

Decolorization of certain dyes, mainly azo, with activated hydrogen peroxide in heterogeneous systems, using different insoluble catalysts with Cu(II) was already studied [26,27,36,37]. The activation of hydrogen peroxide by heterogeneous catalysts was attributed to the formation of highly active hydroxyl radicals [23]. High concentrated H_2O_2 solutions undergo self quenching of $\cdot OH$ radicals, with formation of hydroperoxyl radicals $HO_2\cdot$. Although $HO_2\cdot$ is an effective oxidant itself, its oxidation potential is much lower than that of $\cdot OH$ radicals [37]

$$H_2O_2 + \cdot OH \rightarrow HO_2\cdot + H_2O \tag{6}$$

$$HO_2\cdot + \cdot OH \rightarrow H_2O + O_2 \tag{7}$$

This could explain why increasing H_2O_2 concentration above a certain limit does not always intensify the decolorization.

3.4. *Investigation of the OG azo dye decolorization by UV–vis spectrometry*

The changes of the absorption bands reflect the evolution of the chromophores of OG and useful information could be provided by the analysis of the UV–vis spectra. The UV–vis spectral changes as a function of reaction time of H_2O_2 and of the catalyst are shown in Fig. 6.

The UV–vis spectrum of the untreated initial solution of OG recorded at pH = 7.0 (Fig. 6) shows one main absorption band at 485 nm, which corresponds to the $n \rightarrow \pi^*$ transition of the azo bond (–N=N–), and other two absorption bands at 230 nm and 310 nm, attributed to the $\pi \rightarrow \pi^*$ transition of benzene and naphthalene rings, respectively [38]. The main band at 485 nm was used to monitor the decolorization of OG with H_2O_2 and Cu(II)-A catalyst. As Fig. 6 shows, absorption band at 485 nm disappears after 30 min. The absence of this absorption band indicates the cleavage of azo chromophore during the treatment of the dye solution and proves that OG dye is completely decolorized by H_2O_2/Cu(II)-A system.

3.5. *Effect of OG concentration*

The variation of the decolorization efficiency of the OG dye with H_2O_2 and Cu(II)-A catalyst as a function of reaction time and the initial dye concentration has also been tested (Fig. 7).

As Fig. 7 shows, the decolorization efficiency decreased with increasing OG concentration from 50 to 177 mg L^{-1}, for all

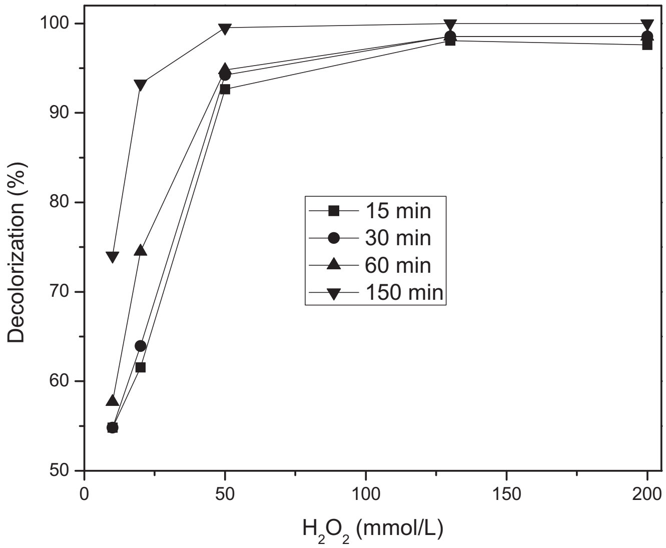

Fig. 5. Effect of H_2O_2 initial concentration and reaction time on the decolorization of OG. Experimental conditions: pH = 7, $[OG]_0 = 50$ mg L^{-1}, 0.06 g catalyst, 24 °C.

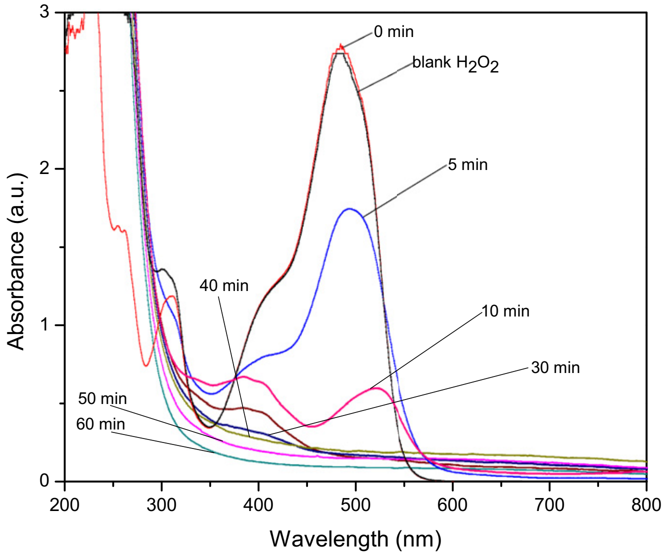

Fig. 6. UV–Vis spectra of OG water solutions during the treatment process with Cu(II)-A/H_2O_2. Experimental conditions: $[OG]_0 = 50$ mg L^{-1}; $[H_2O_2]_0 = 130$ mmol L^{-1}; 0.06 g catalyst; pH = 7; 24 °C.

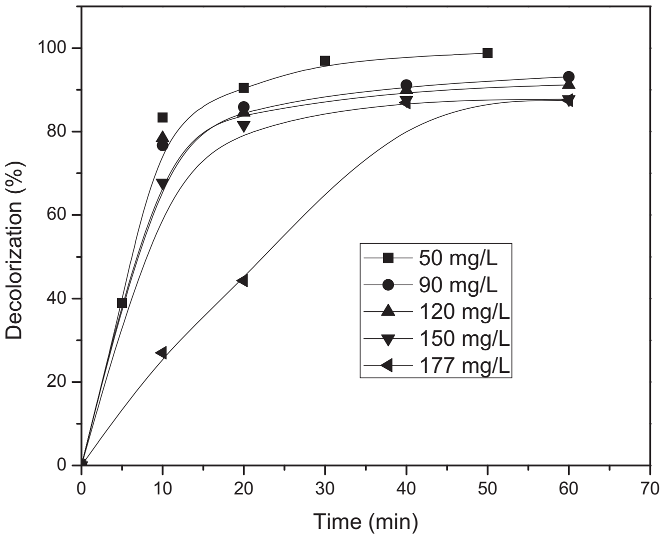

Fig. 7. Effect of reaction time and OG concentration on the decolorization of OG. Experimental conditions: 0.06 g catalyst; pH = 7, 24 °C).

investigated reaction time. At the lowest concentration (50 mg L^{-1}), at room temperature, the solution is completely discolored after 40 min. In the more concentrated OG solution (177 mg L^{-1}) the process develops relatively slowly and the decolorization degree reaches 87.5% after 40 min. This behavior can be ascribed to the limited number of $\cdot$OH radicals involved in the decolorizing process.

3.6. Effect of temperature

The catalyst Cu(II)-A was tested at pH = 7 for different concentrations of the OG dye, after 60 min of reaction time, at three temperatures: 24 °C, 35 °C and 50 °C (Fig. 8).

As Fig. 8 shows, the decolorization degree decreased with the increase of the dye concentration, for the same temperature. On the other hand, the decolorization efficiency increased with the raising of temperature, for the studied dye concentrations, except $[OG]_0 = 50$ mg L^{-1}, when the decolorization degree do not show any temperature influence. Probably, as temperature increase the production of oxidizing species, such as $\cdot$OH, was favorized because of the increase of reaction rate.

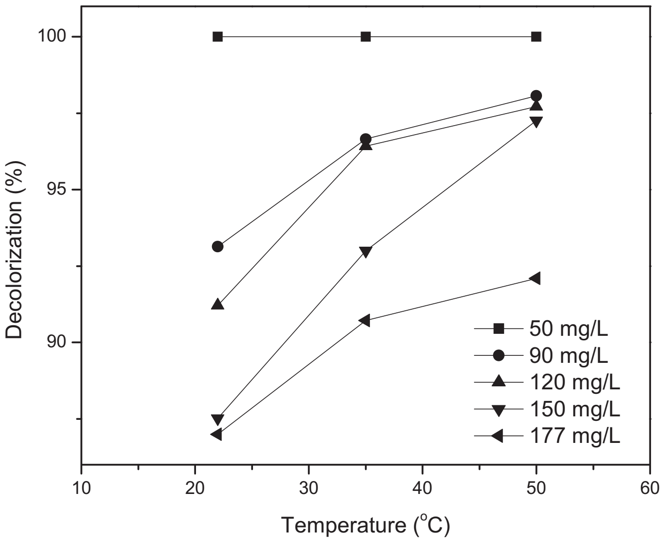

Fig. 8. Effect of temperature and OG concentration on the decolorization of OG. Experimental conditions: pH = 7; $[H_2O_2] = 130$ mmol L^{-1}; 0.06 g Cu(II)-A; reaction time 60 min).

3.7. Effect of the amount of catalyst

The amount of catalyst is an important parameter for the OG decolorization and for the decolorization efficiency. This effect was studied by varying the amount of catalyst from 0.01 g to 0.06 g in the following optimal conditions: pH = 7, $[H_2O_2]_0 = 130$ mmol L^{-1}, $[OG]_0 = 50$ mg L^{-1} (Fig. 9).

As Fig. 9 shows, increasing the amount of catalyst leads to a shorter time for decolorization. For the smallest amount tested (0.01 g) the decolorization percent is 95% after 55 min and more than 99% decolorization is reached after 85 min. When the amount of Cu(II)-A varied between 0.02 and 0.04 g, slight differences can be noticed, almost the same variation of decolorization degree being obtained. For 0.06 g catalyst a decolorization efficiency of 99% is reached after 25 min and a maximum of 100% after 60 min of treatment. The increase in the catalyst amount can contribute to the increased rate of formation of $\cdot$OH radicals, and therefore the decolorization efficiency increases.

3.8. The catalyst stability

The stability of the catalyst has been tested following the amount of Cu(II) ions released in the solution after decolorization with Cu(II)-A/H_2O_2 and the results are summarized in Table 3.

In the conditions of temperature and dye concentration given in Table 3, the catalyst Cu(II)-A showed a good stability, after 60 min of decolorization the amount of Cu(II) released in the solution does not exceed 5.3%. For the same temperature a slight increase of the amount of Cu(II) released in solution with the increase of the dye concentration is observed. This is probably due to the formation of a larger amount of reaction products, affecting the stability of the catalyst. Also, the increase of the amount of Cu(II) released in solution with the increase of temperature, for the same dye concentration, takes place.

3.9. Mineralization of dye

The reaction intermediates obtained during the oxidation of azo dyes could be stable and even more toxic than the initial dye [1],

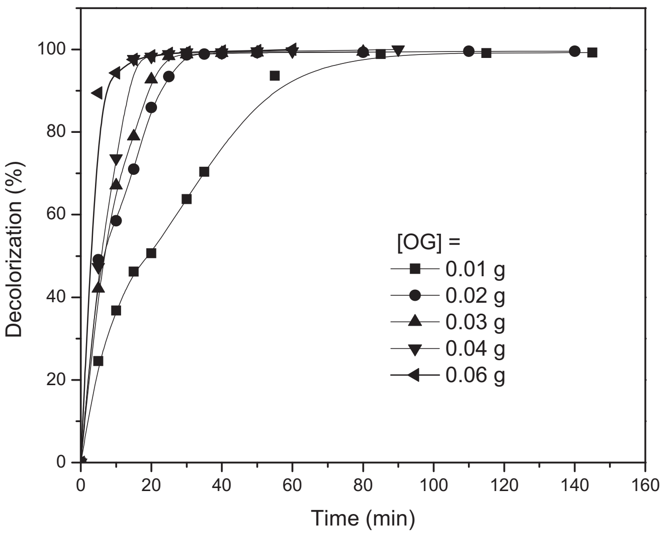

Fig. 9. Effect of the catalyst amount on the decolorization of OG. Experimental conditions: pH 7.00, $[H_2O_2]_0 = 130$ mmol L^{-1}, $[OG]_0 = 50$ mg L^{-1}.

Table 3
Cu(II) ions released in the dye solution after 60 min at different temperatures and initial dye concentrations.

Temperature (°C)	Cu(II) released, %				
	$[OG]_0$, mg L^{-1}				
	89	120	150	177	226
24	3.2	4.2	4.2	4. 7	4.8
35	3.4	4.2	4.2	4. 9	5.0
50	3.9	4.4	4.5	5.1	5.3

therefore the products resulting from the mineralization of the dye need to be investigated. The total or partial transformation of certain dyes in CO_2 in heterogeneous catalysis was already reported [27,39]. We propose the following stoichiometric equation for the total mineralization of the OG by ·OH:

$$C_{16}H_{10}N_2O_7S_2^{2-} + 84\cdot OH = 16CO_2 + 2NO_3^- + 2SO_4^{2-} + 4H^+ + 45H_2O \tag{8}$$

It is worth noting that during the decolorization of the OG solution using H_2O_2 a significant effervescence occurred. The mineralization process of OG is indicated through certain preliminary tests, such as trapping the resulted CO_2 and TOC analysis.

CO_2 was determined by trapping the gaseous products of reaction in a $Ba(OH)_2$ solution and by determining the resulted $BaCO_3$ gravimetrically [32]. For a sample of 0.03 g commercial dye, at 50 °C after 3 h 0.1829 g $BaCO_3$ were obtained, that corresponding to 92.2% C released as CO_2.

However, TOC analysis is more accurate and appropriate method for evaluating the decontamination of polluted waters containing organics, since it takes into account all the residual carbon contained in the reaction products [15].

The TOC removal ratio (TOC_r) is defined as follows (Eq. (9)):

$$TOC_r = \left(1 - \frac{TOC_t}{TOC_0}\right) \times 100 \tag{9}$$

where TOC_0 and TOC_t are the TOC values at the initial moment and at the time t, respectively.

In Table 4 are summarized the values of TOC_r for two dye solutions of concentration 50 and 100 mg L^{-1}, discolored at 22 °C and 50 °C and different reaction time.

As Table 4 shows, TOC_r increased with the increase of the temperature and the reaction time, for the same $[OG]_0$. For the most dilute solution (50 mg L^{-1}), after 35 min at 22 °C, TOC_r was only ~20%, probably due to the partial transformation of the dye and the relatively short time to action of the oxidizing system. After 150 min at 22 °C, the longer reaction time enables dye mineralization, a TOC_r of about 73% being observed. Increasing $[OG]_0$ at 100 mg L^{-1}, after 210 min at 50 °C, an increase of the TOC_r up to 92% can be noticed, even 100% decolorization occurred. The mineralization of OG to CO_2 and H_2O, depends on the reaction time and temperature, due to reaction intermediates which can be formed during oxidation.

Table 4
TOC removal ratio on the mineralization of OG solutions with different initial concentration, discolored at 22 °C and 50 °C and different reaction time.

$[OG]_0$, (mg L^{-1})	22 °C		50 °C	
	Time (min)	TOC removal ratio (%)	Time (min)	TOC removal ratio (%)
50	35	19.9	35	53.8
	150	72.8	150	94.4
100	150	85.3	65	88.2
	210	87.7	210	91.8

3.10. Decolorization kinetics

In order to investigate the reaction kinetics, the decolorization of OG with H_2O_2 and Cu(II)-A was conducted with five different initial dye concentration (C_1 = 50 mg L^{-1}; C_2 = 90 mg L^{-1}; C_3 = 120 mg L^{-1}; C_4 = 150 mg L^{-1}; C_5 = 177 mol L^{-1}), each one at three different temperatures (24 °C, 35 °C and 50 °C). Catalyst and H_2O_2 concentrations were kept constant, 0.06 g Cu(II)-A, 130 mmol L^{-1} H_2O_2 and the pH was set to 7.

For each experiment, absorption spectra in the 400–700 nm range were recorded at different time intervals. After calibration, the time dependence of the dye concentration in the solution was calculated.

The obtained kinetic curves were normalized by converting them into the time dependence of the conversion degree α, defined as:

$$\alpha(t) = \frac{C_0 - C(t)}{C_0} \tag{10}$$

where C_0 and $C(t)$ are the dye concentrations at the initial moment and at time t, respectively.

In formal kinetics, the reaction order model provides the following equations for the time dependence of the conversion degree:

$$(1-\alpha)^{1-n} = 1 - (n-1)C_0^{n-1} \times k_n t \quad \text{for} \quad n \neq 1 \tag{11}$$

$$(1-\alpha) = \exp(-k_1 t) \quad \text{for} \quad n = 1 \tag{12}$$

where k_n is the rate constant and n the reaction order.

The time dependence of the conversion degree at different temperature and for four different initial dye concentrations is shown in Fig. 10.

As it is obvious in Fig. 10, the experimental time dependence of the conversion degree was almost independent of the initial dye concentration at all three temperatures. The results show that, with H_2O_2 in considerable excess (130 mmol L^{-1}), the decolorization of OG with H_2O_2 and Cu(II)-A follows the pseudo-first-order kinetics, described by Eq. (12). By nonlinear regression of the experimental data (continuous curves in Fig. 10) the values of the effective rate constant k_1 were evaluated as a function of temperature, as follows: 0.1311 min^{-1}, 0.1726 min^{-1}, and 0.2513 min^{-1} at 24 °C, 35 °C, and 50 °C, respectively. These values were used in the following to estimate the activation parameters.

3.11. Activation parameters

The apparent activation energy was calculated using the linear form of the Arrhenius equation:

$$\ln k = \ln A - \frac{E_a}{R}\frac{1}{T} \tag{13}$$

where k is the rate constant, A is pre-exponential factor, E_a is the activation energy, T is the absolute temperature and R is the universal gas constant.

The activation enthalpy and the entropy were calculated using the Eyring equation in the thermodynamic formulation [40,41]:

$$k = \frac{k_B T}{h}\exp\left(-\frac{\Delta H^{\neq}}{RT}\right)\exp\left(\frac{\Delta S^{\neq}}{R}\right) \tag{14}$$

where $\Delta H^{\neq}$ is the activation enthalpy, k_B is the Boltzmann constant, h is the Planck constant and $\Delta S^{\neq}$ is the activation entropy. Eq. (14) can be linearized in the following form:

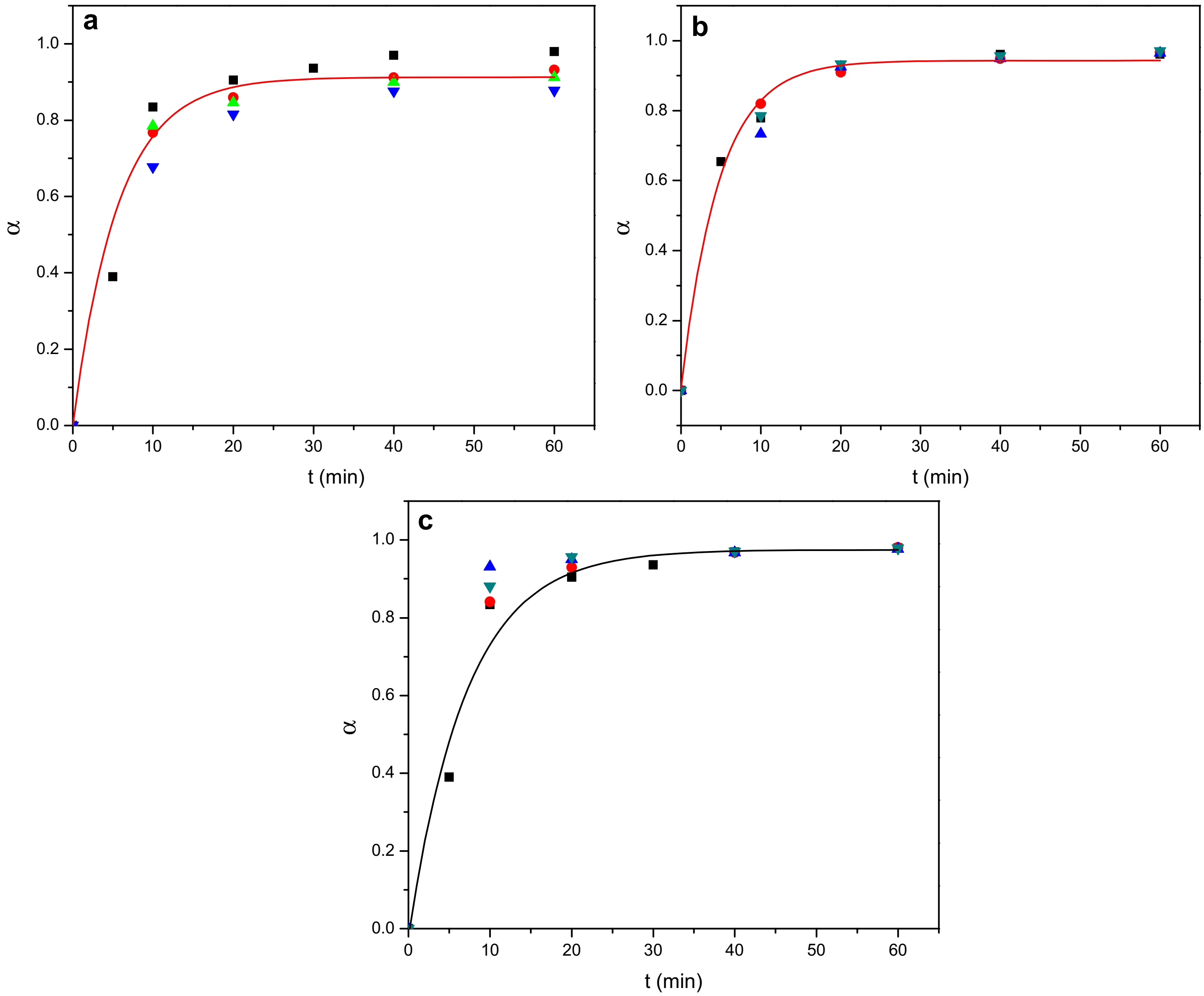

Fig. 10. Time dependence of the conversion degree at 24 °C (a), 35 °C (b) and 50 °C (c), for five different initial dye concentrations: ● - 50 mg L^{-1}; ■ – 90 mg L^{-1}; ▲ – 120 mg L^{-1}; ▼ – 150 mg L^{-1}.

$$\ln\frac{k}{T} = \ln\frac{k_B}{h} + \frac{\Delta S^{\neq}}{R} - \frac{\Delta H^{\neq}}{R}\frac{1}{T} = \text{const} - \frac{\Delta H^{\neq}}{R}\frac{1}{T} \qquad (15)$$

Linear regressions of ln $k = f(1/T)$ and of $\ln(k/T) = f(1/T)$ are shown in Fig. 11.

The value of the apparent activation energy estimated from the linear regression in Fig. 11 is $E_a = 20$ kJ mol^{-1}. This is a rather low value, if taken into account that, for example, OG decolorization in aqueous solution by Fenton oxidation has $E_a = 34.84$ kJ mol^{-1} [21], leading us to the conclusion that Cu(II)-A is a more efficient catalyst than Fe(II) in dye oxidation with peroxide.

Linear regression of the $\ln(k/T) = f(1/T)$, shown in Fig. 11, allowed the calculation of the activation enthalpy and entropy values as $\Delta H^{\neq} = 17.4$ kJ mol^{-1} and $\Delta S^{\neq} = -203.2$ J mol^{-1} K^{-1}. Again, the activation enthalpy has a rather low value, suggesting that the transition state complex is stabilized by energy lowering effects, an observation that correlates with the similar conclusion on the activation energy. This result suggests that the high efficiency of the Cu(II)-A catalyst in OG oxidation with peroxide can be explained by a stabilization of the activated complex on the catalyst surface. The

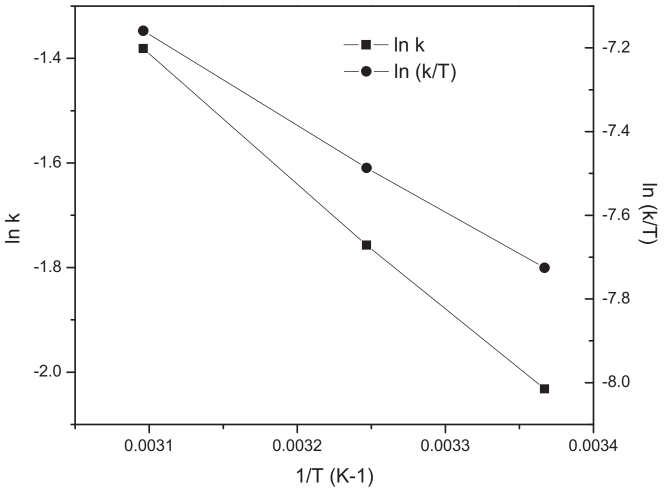

Fig. 11. Linear regressions of experimental data.

Table 5
Comparative results of OG decolorization and degradation by various methods.

Decolorization system	Optimum conditions of reaction	Dye concentration	Observations	Ref.
Fenton-like system	pH = 2.5 $[H_2O_2] = 100$ mg L^{-1} $[Fe^{3+}] = 1$ mg L^{-1}	45 mg L^{-1}	100% after 480 min 31% TOC	[23]
D. squalens strain white rot	In Kirk medium, and static cultivation	500 mg L^{-1}	~95% in 14 days	[14]
Nano-sized Sn(IV)/TiO_2/AC photocatalyst	pH = 2.00 $[H_2O_2] = 1.5$ mL L^{-1}, $[TiO_2] = 12.5$ g L^{-1} Light source-300 W	50 mg L^{-1}	99.1% after 60 min $E_a = 34.84$ kJ mol^{-1}	[18]
Electrochemical removal	pH = 9.0 0.017 M NaCl Graphite electrode at 11.72 mA cm^{-2}	100 mg L^{-1}	100% after 60 min	[6]
Iron-nickel bimetallic nanoparticles	Nanocatalyst loading – 3 g L^{-1} (size of 20–40 nm)	150 mg L^{-1}	100%, after 10 min	[42]
Fenton reactions	pH = 2.5–3.0 $H_2O_2 = 10^{-2}$ M $[H_2O_2]/[Fe^{2+}] = 286:1$.	10–50 mg L^{-1}	>94.6% after 60 min	[24]
Sonophotocatalytic oxidation using a heterogeneous photocatalyst TiO_2	Ultrasound irradiation at a frequency of 213 kHz and TiO_2 1 mg mL^{-1}	40 mg L^{-1}	82% TOC after 4 h at pH 5.8 and 60% at pH 12	[43]
Persulfate/Fe^{2+} reagent	pH = 3.5 [persulfate = 4 mM] $[Fe^{2+}] = 4$ mM	45 mg L^{-1}	99% after 30 min $E_a = 92.2$ kJ mol^{-1}	[44]
Cu(II)-chelating macroporous resin functionalized with DETA	pH = 7 $H_2O_2 = 130$ mmol L^{-1} 0.06 g catalyst	50–177 mg L^{-1}	100% after 60 min $E_a = 20$ kJ mol^{-1} $TOC_r = 94\%$, 50 °C, after 150 min reaction time, $[OG]_0 = 50$ mg L^{-1}	In this article

lower value of activation enthalpy is thus indicative of higher catalytic efficiency, and for the sake of comparison we mention the reported values for the heterogeneous catalyzed oxidative decolorization of pyrocatechol violet [27] by hydrogen peroxide catalyzed with copper complexes, when the activation enthalpy and the entropy were $\Delta H^{\neq} = 61{,}15$ kJ mol^{-1}; $\Delta S^{\neq} = -60$ J mol^{-1} K^{-1}. The value of $\Delta S^{\neq}$ implies a rigidity of the reacting dye molecules, so that they react only in certain reduced number of states or geometrical orientations.

Some literature data on decolorization and mineralization of OG dye by different methods, comparative with that obtained in this paper, are summarized in Table 5.

As Table 5 shows, almost all the parameters tested for the catalytic system used in this paper are more effective than those of the previously reported methods: a large range of dye concentration, 50–177 mg L^{-1}, mild conditions (pH = 7), small amount of catalyst (0.06 g Cu(II)-A), for 130 mmol L^{-1} H_2O_2, low activation energy ($E_a = 20$ kJ mol^{-1}), with an advanced color removal achieved in 60 min at 24 °C. The mineralization efficiency, expressed by TOC_r, increased from 73 to 94%, with the temperature increase from 24 to 50 °C, respectively, after 150 min reaction time and $[OG]_0 = 50$ mg L^{-1}.

4. Conclusions

The oxidative decolorization of OG, in the presence of a heterogeneous system involving hydrogen peroxide and a new catalyst obtained by the adsorption of Cu(II) ions onto a macroporous chelating polymer functionalized with DETA, has been studied in this paper. The effect of pH, H_2O_2 and dye concentration, reaction time, temperature and the amount of catalyst on the decolorization efficiency of OG containing waters has been investigated in detail. On the basis of the evaluation of the experimental results following optimal conditions are established: $[OG]_0 = 50–177$ mg L^{-1}, pH = 7, $[H_2O_2] = 130$ mmol L^{-1}, 1.2 g L^{-1} Cu(II)-A catalyst, at which complete color removal was achieved in 60 min at 24 °C.

The mineralization degree of OG dye is favored by the increase of temperature and decreases with increasing dye concentration. The decolorization and mineralization degree of OG dye is favored by the increase of temperature, with maximum TOC removal ratio of 94% at 50 °C for dye solution of 50 mg L^{-1}. The values of activation energy ($E_a = 20$ kJ mol^{-1}), activation enthalpy ($\Delta H^{\neq} = 17.4$ kJ mol^{-1}), and entropy ($\Delta S^{\neq} = -203.2$ J mol^{-1} K^{-1}), lower comparative with literature data, showed that the oxidative process requires a small amount of energy and has an endothermic nature, and demonstrated a high catalytic efficiency of this system. The high efficiency of the Cu(II)-A catalyst in OG oxidation with peroxide can be explain by the formation of an activated complex on the catalyst surface. The Cu(II)-A catalyst has been successfully employed in advanced oxidation process applied to decolorization of aqueous solution of the azo dye orange G; this system constitutes a simple and effective method compared to those previously reported for the degradation of orange G.

Acknowledgments

The financial support of this research by the Grant No. 313/2011 (Exploratory Research Project) is gratefully acknowledged.

References

[1] Golka K, Kopps S, Myslak ZW. Carcinogenicity of azo colorants: influence of solubility and bioavailability. Toxicol Lett 2004;151:203–10.

[2] Pearce CI, Lloyd JR, Guthrie JT. The removal of colour from textile wastewater using whole bacterial cells: a review. Dyes Pigm 2003;58:179–96.

[3] Kaushik P, Malik A. Fungal dye decolourization: recent advances and future potential. Environ Int 2009;35:127–41.

[4] Soon AN, Hameed BH. Heterogeneous catalytic treatment of synthetic dyes in aqueous media using Fenton and photo-assisted Fenton process. Desalination 2011;269:1–16.

[5] Aksu Z. Application of biosorption for the removal of organic pollutants: a review. Process Biochem 2005;40:997–1026.

[6] Muthukumar M, Karuppiah MT, Raju GB. Electrochemical removal of CI acid orange 10 from aqueous solutions. Sep Purif Technol 2007;55:198–205.

[7] Forgacs E, Cserháti T, Oros G. Removal of synthetic dyes from wastewaters: a review. Environ Int 2004;30:953–71.

[8] Anjaneyulu Y, Sreedhara Chary N, Samuel Suman Raj D. Decolourization of industrial effluents – available methods and emerging technologies – a review. Rev Environ Sci Biotechnol 2005;4:245–73.

[9] Kolekar YM, Pawar SP, Gawai KR, Lokhande PD, Shouche YS, Kodam KM. Decolorization and degradation of Disperse Blue 79 and Acid Orange 10, by *Bacillus fusiformis* KMK5 isolated from the textile dye contaminated soil. Bioresour Technol 2008;99:8999–9003.

[10] Chen C, Chen J, Ni W, Tian X, Huang F. Biodegradation of Orange G by wood-rot fungi *Phanerochaete sordida* TXJ-1302A and *Tyromyces lauteus* TXJ-1302B. Bioresour Technol 2008;99:3926–9.

[11] Eichlerová I, Homolka L, Nerud F. Ability of industrial dyes decolorization and ligninolytic enzymes production by different *Pleurotus* species with special attention on *Pleurotus calyptratus*, strain CCBAS 461. Process Biochem 2006; 41:941–6.

[12] Eichlerová I, Homolka L, Nerud F. Synthetic dye decolorization capacity of white rot fungus *Dichomitus squalens*. Bioresour Technol 2006;97:2153–9.

[13] Eichlerová I, Homolka L, Nerud F. Decolorization of high concentrations of synthetic dyes by the white rot fungus *Bjerkandera adusta* strain CCBAS 232. Dyes Pigm 2007;75:38–44.

[14] Eichlerová I, Homolka L, Benada O, Kofroňová O, Hubálek T, Nerud F. Decolorization of Orange G and Remazol Brilliant Blue R by the white rot fungus *Dichomitus squalens*: toxicological evaluation and morphological study. Chemosphere 2007;69:795–802.

[15] Lachheb H, Puzenat E, Houas A, Ksibi M, Elaloui E, Guillard C, et al. Photocatalytic degradation of various types of dyes (Alizarin S, Crocein Orange G, Methyl Red, Congo Red, Methylene Blue) in water by UV-irradiated titania. Appl Catal B Environ 2002;39:75–90.

[16] Sökmen M, Özkan A. Decolourising textile wastewater with modified titania: the effects of inorganic anions on the photocatalysis. J Photochem Photobiol 2002;A 147:77–81.

[17] Nagaveni K, Sivalingam G, Hegde MS, Madras G. Solar photocatalytic degradation of dyes: high activity of combustion synthesized nano TiO_2. Appl Catal B Environ 2004;48:83–93.

[18] Sun J, Wang X, Sun J, Sun R, Sun S, Qiao L. Photocatalytic degradation and kinetics of Orange G using nano-sized Sn(IV)/TiO_2/AC photocatalyst. J Mol Catal A Chem 2006;260:241–6.

[19] Kwon JM, Kim YH, Song BK, Yeom SH, Kim BS, Im JB. Novel immobilization of titanium dioxide (TiO_2) on the fluidizing carrier and its application to the degradation of azo-dye. J Hazard Mater 2006;134:230–6.

[20] Vinu R, Madras G. Synthesis and photoactivity of Pd substituted nano-TiO_2. J Mol Catal A Chem 2008;291:5–11.

[21] Sun J, Qiao L, Sun S, Wang G. Photocatalytic degradation of Orange G on nitrogen-doped TiO_2 catalysts under visible light and sunlight irradiation. J Hazard Mater 2008;155:312–9.

[22] Xie YB, Li XZ. Interactive oxidation of photoelectrocatalysis and electro-Fenton for azo dye degradation using TiO_2-Ti mesh and reticulated vitreous carbon electrodes. Mater Chem Phys 2006;95:39–50.

[23] Hsueh L, Huang YH, Wang CC, Chen CY. Degradation of azo dyes using low iron concentration of Fenton and Fenton-like system. Chemosphere 2005;58: 1409–14.

[24] Sun SP, Li CJ, Sun JH, Shi SH, Fan MH, Zhou Q. Decolorization of an azo dye Orange G in aqueous solution by Fenton oxidation process: effect of system parameters and kinetic study. J Hazard Mater 2009;161:1052–7.

[25] Shah V, Verma P, Stopka P, Gabriel J, Baldrian P, Nerud F. Decolorization of dyes with copper(II)/organic acid/hydrogen peroxide systems. Appl Catal B Environ 2003;46:287–92.

[26] Salem IA. Activation of H_2O_2 by Amberlyst-15 resin supported with copper(II)- complexes toward oxidation of crystal violet. Chemosphere 2001;44: 1109–19.

[27] Gemeay AH, Mansour IA, El-Sharkawy RG, Zaki AB. Kinetics and mechanism of the heterogeneous catalyzed oxidative degradation of indigo carmine. J Mol Catal A Chem 2003;193:109–20.

[28] Gemeay AH, Mansour IA, El-Sharkawy RG, Zaki AB. Kinetics of the oxidative degradation of thionine dye by hydrogen peroxide catalyzed by supported transition metal ions complexes. J Chem Technol Biotechnol 2004;79:85–96.

[29] Aravindhan R, Fathima NN, Rao JR, Nair BU. Wet oxidation of acid brown dye by hydrogen peroxide using heterogeneous catalyst Mn-salen-Y zeolite: a potential catalyst. J Hazard Mater 2006;138:152–9.

[30] Maxim S, Flondor A, Bunia I, Luca C. Acrylic three dimensional netwoks-I. Copolymers with acrylamidoalkylenamine functional groups. Eur Polym J 1998;34:1379–85.

[31] Dulman V, Simion C, Bârsănescu A, Bunia I, Neagu V. Adsorption of anionic textile dye Acid Green 9 from aqueous solution onto weak or strong base anion exchangers. J Appl Polym Sci 2009;113:615–27.

[32] Welcher FJ. Standard methods of chemical analysis. Krieger Pub Co; 1962.

[33] Lanigan KC, Pidsosny K. Reflectance FTIR spectroscopic analysis of metal complexation to EDTA and EDDS. Vib Spectrosc 2007;45:2–9.

[34] Wu KH, Wang YR, Hwu WH. FTIR and TGA studies of poly(4-vinylpyridine co divinylbenzene) Cu(II) complex. Polym Degrad Stabil 2003;79:195–200.

[35] Simpson JA, Cheeseman KH, Smith SE, Dean RT. Free-radical generation by copper ions and hydrogen peroxide. Stimulation by Hepes buffer. Biochem J 1988;254:519–23.

[36] Šuláková R, Hrdina R, Soares GMB. Oxidation of azo textile soluble dyes with hydrogen peroxide in the presence of Cu(II)-chitosan heterogeneous catalysts. Dyes Pigm 2007;75:19–24.

[37] Fathima NN, Aravindhan R, Rao JR, Nair BU. Dye house wastewater treatment through advanced oxidation process using Cu-exchanged Y zeolite: a heterogeneous catalytic approach. Chemosphere 2008;70:1146–51.

[38] Li G, Qu J, Zhang X, Liu H, Liu H. Electrochemically assisted photocatalytic degradation of Orange II: influence of initial pH values. J Mol Catal A Chem 2006;259:238–44.

[39] Neamtu M, Siminiceanu I, Yediler A, Kettrup A. Kinetics of decolorization and mineralization of reactive azo dyes in aqueous solution by the UV/H_2O_2 oxidation. Appl Catal B Environ 2004;51:149–57.

[40] Winzor DJ, Jackson CM. Interpretation of the temperature dependence of equilibrium and rate constants. J Mol Recognit 2006;19:389–407.

[41] Eyring H. The activated complex in chemical reactions. J Chem Phys 1935;3: 107–15.

[42] Bokare AD, Chikate RC, Rode CV, Paknikar KM. Iron–nickel bimetallic nanoparticles for reductive degradation of azo dye Orange G in aqueous solution. Appl Catal B Environ 2008;79:270–8.

[43] Madhavan J, Grieser F, Ashokkumar M. Degradation of orange-G by advanced oxidation processes. Ultrason Sonochem 2010;17:338–43.

[44] Xu XR, Li XZ. Degradation of azo dye Orange G in aqueous solutions by persulfate with ferrous ion. Sep Purif Technol 2010;72:105–11.